

# Antioxidant phenolic esters with potential anticancer activity: solution equilibria studied by Raman spectroscopy

N. F. L. Machado,<sup>a</sup> R. Calheiros,<sup>a</sup> A. Gaspar,<sup>a</sup> J. Garrido,<sup>a,b</sup> F. Borges<sup>a,c</sup> and M. P. M. Marques<sup>a,d\*</sup>



The solution Raman pattern of a series of structurally related hydroxycinnamic and hydroxybenzoicesters (caffeates and gallates) with potential antioxidant/anticancer activity was studied, for different biologically significant concentrations. The spectra were assigned with the help of theoretical calculations in the light of previously reported experimental data for these compounds in the solid state. Evidence of the formation of dimeric entities in solution, via  $(C)=O \cdots H(O)$  and/or  $(C)=O \cdots H(C)$  intermolecular hydrogen bonds, was obtained. The dimer-to-monomer equilibrium, which influences the antioxidant activity of this kind of systems, was monitored through Raman titration experiments. Copyright © 2008 John Wiley & Sons, Ltd.

Supporting information may be found in the online version of this article.

**Keywords:** Raman spectroscopy; hydroxycinnamic; hydroxybenzoic; antioxidant; chemopreventive

## Introduction

Polyphenolic compounds are nowadays recognized to possess encouraging biological properties, with huge relevance either in food or health sciences.<sup>[1–5]</sup> In particular, phenolic antioxidant compounds are capable of preventing or inhibiting carcinogenesis at different levels, by distinct mechanisms, thereby reducing the risk and/or progression of certain types of cancer.<sup>[6,7]</sup> Accordingly, a growing interest in phenolic antioxidant agents is emerging, aiming at the prevention of numerous diseases mainly caused by the occurrence of deleterious free radical species.<sup>[6,8–12]</sup>

For phenolic acid derivatives such as hydroxycinnamic and hydroxybenzoic *n*-alkyl esters, either of natural or synthetic origin, the presence of the ring substituent hydroxyl groups is known to be an essential chemical feature for their particular biological profile, while the influence of the nature of both the pendant carbon chain and the ester moiety is still controversial.<sup>[7,10–14]</sup> Understanding the molecular basis of the antioxidant capacity of these systems, in order to clarify the strong structural dependence of their activity, is essential for a rational design of efficient polyphenolic chemopreventive agents.

Phenolic derivatives are known to yield dimeric entities in condensed phases<sup>[15,16]</sup> via intermolecular hydrogen-bond-type interactions. The relative importance of intra- versus intermolecular H-bonds has proved to be the determinant of the conformational preferences of these compounds both in the solid state and in solution, which, in turn, rule their biological role. Actually, the hydroxyl ring substituent groups, which are mainly responsible for the antioxidant and antiproliferative properties of these systems, are involved in  $(C)=O \cdots H(O)$  and  $(C)=O \cdots H(C)$  intermolecular close contacts when dimers are formed. When this occurs, the reductive capacity of the phenols is hindered. Consequently, the percentage of monomeric versus dimeric

species in a pharmacological solution will strongly determine its activity.

Since the biological function of phenolic antioxidant agents is usually evaluated in solution (often in dimethylsulfoxide (DMSO)), it is of the utmost importance to have an exact knowledge of the predominant species present in these conditions, in a pharmacologically significant concentration range (ca  $1.0 \times 10^{-2}$  to  $1.0 \text{ mol dm}^{-3}$ ). The present study aims at achieving this goal by carrying out a Raman spectroscopy study in solution of several variable-length alkyl phenolic esters, as well as the parent acids (caffeic and gallic acid and its derivatives, Fig. 1): methyl *trans*-3-(3,4-dihydroxyphenyl)-2-propenoate (methyl caffeate (MC)), ethyl *trans*-3-(3,4-dihydroxyphenyl)-2-propenoate (ethyl caffeate (EC)), propyl *trans*-3-(3,4-dihydroxyphenyl)-2-propenoate (propyl caffeate (PC)), isopropyl *trans*-3-(3,4-dihydroxyphenyl)-2-propenoate (isopropyl caffeate (IPC)), butyl *trans*-3-(3,4-dihydroxyphenyl)-2-propenoate (butyl caffeate (BC)), octyl *trans*-3-(3,4-dihydroxyphenyl)-2-propenoate (octyl caffeate (OC)), dodecyl *trans*-3-(3,4-dihydroxyphenyl)-2-propenoate (dodecyl caffeate (DC)), methyl 3,4,5-trihydroxybenzoate (methyl

\* Correspondence to: M. P. M. Marques, Departamento de Bioquímica, Faculdade de Ciências e Tecnologia, Universidade de Coimbra, Apartado 3126, 3001-401 Coimbra, Portugal. E-mail: pmc@ci.uc.pt

a Unidade I&D "Química-Física Molecular", Faculdade de Ciências e Tecnologia, Universidade de Coimbra, 3000 Coimbra, Portugal

b Departamento de Engenharia Química, Instituto Superior de Engenharia do Porto, 4200-072 Porto, Portugal

c Departamento de Química Orgânica, Faculdade de Farmácia, Universidade do Porto, 4050-047 Porto, Portugal

d Departamento de Bioquímica, Faculdade de Ciências e Tecnologia, Universidade de Coimbra, Ap. 3126, 3001-401 Coimbra, Portugal

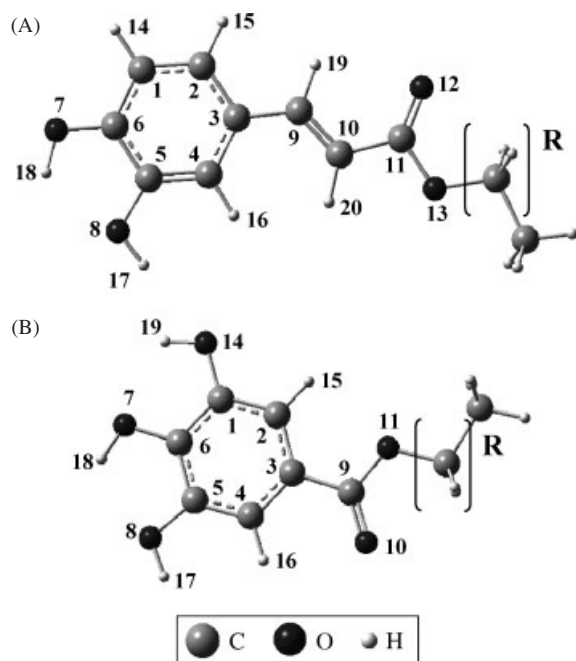


**Figure 1.** Schematic representation of the hydroxyphenolic esters studied in the present work (most stable calculated geometries). (A) hydroxycinnamates (caffeates). (B) Gallates.  $R = (\text{CH}_2)_n$ ,  $n = 0, 1, 2, 3, 7, 11$  for methyl, ethyl, propyl, butyl, octyl and dodecyl esters, respectively;  $R = (\text{CHCH}_3)$  for isopropyl esters. (The atom numbering is included, with the exception of the alkyl ester group. The structure in A refers to a *S-cis/anti* conformation, while the one in B represents a *S-cis/syn* conformation).

gallate (MG)), ethyl-3,4,5-trihydroxybenzoate (ethyl gallate (EG)), isopropyl-3,4,5-trihydroxybenzoate (isopropyl gallate (IPG)) and dodecyl-3,4,5-trihydroxybenzoate (dodecyl gallate (DG)). The monomer-to-dimer equilibrium was also investigated through Raman titration experiments.

The results obtained were interpreted in the light of the theoretical vibrational spectra presently determined for the systems studied. Moreover, they were compared with previously obtained experimental Raman data in the solid state,<sup>[16]</sup> and with the calculated structural parameters and vibrational wavenumbers for analogous systems.<sup>[15,17–20]</sup>

## Experimental

### Chemicals

*Trans*-caffeic acid (CA), gallic acid, methyl-, ethyl-, propyl-, butyl-, octyl- and dodecyl gallates were purchased from Sigma-Aldrich Química S.A. (Sintra, Portugal). DMSO- $d_6$  (99.8%) was obtained from E. Merck, Darmstadt, Germany. All other reagents and solvents were *pro analysis* grade, purchased from Merck (Lisbon, Portugal) or Sigma-Aldrich Química S.A. (Sintra, Portugal).

The phenolic esters under study were synthesized according to previously reported procedures.<sup>[13–15,21]</sup>

### Raman spectroscopy

The Raman spectra were obtained at room temperature in a triple monochromator Jobin-Yvon T64000 Raman system (focal distance 0.640 m, aperture  $f/7.5$ ) with holographic gratings of

1800 grooves/mm. The premonochromator stage was used in the subtractive mode. The detection system was a liquid-nitrogen-cooled non-intensified  $1024 \times 256$  pixel ( $1''$ ) charge coupled device (CCD). The entrance slit was set to 200  $\mu\text{m}$ , and the slit between the premonochromator and the spectrograph was opened to 12 mm.

For some of the samples the spectra were recorded with a Spex Ramalog 1403 double spectrometer (focal distance 0.85 m, aperture  $f/7.8$ ) equipped with holographic gratings of 1800 grooves/mm (in the additive mode) and a detector assembly containing a thermoelectrically cooled Hamamatsu R928 photomultiplier tube. Slits of 320  $\mu\text{m}$  and a resolution of  $1 \text{ cm}^{-1} \text{ s}^{-1}$  were used.

The excitation radiation was provided ( $\sim 100 \text{ mW}$  at the sample position) by the 514.5 nm line of an argon ion laser (Coherent, model Innova 300). A  $90^\circ$  geometry between the incident radiation and the collecting system was employed. Samples were sealed in Kimax glass capillary tubes of 0.8 mm inner diameter. Under the above conditions, the error in wavenumbers was estimated to be within  $1 \text{ cm}^{-1}$ .

### DFT calculations

The quantum mechanical calculations were performed using the Gaussian 03W program,<sup>[22]</sup> within the density functional theory (DFT) approach, in order to properly account for the electron correlation effects (particularly important in this kind of conjugated systems). The widely employed hybrid method denoted by (B3LYP), which includes a mixture of Hartree–Fock (HF) and DFT exchange terms and the gradient-corrected correlation functional of Lee *et al.*,<sup>[23,24]</sup> as proposed and parameterized by Becke,<sup>[25,26]</sup> was used, along with the double-zeta split valence basis set 6-31G\*\*.<sup>[27]</sup>

Molecular geometries were fully optimized by the Bery algorithm, using redundant internal coordinates.<sup>[28]</sup> The bond lengths are accurate to within  $ca$  0.1 pm and the bond angles to within  $ca$   $0.1^\circ$ . The final root-mean-square (rms) gradients were always less than  $3 \times 10^{-4}$  hartree/bohr or hartree/radian. No geometrical constraints were imposed on the molecules under study. The relative energies and populations (Boltzmann distribution at 298.15 K) were calculated for all conformers, using the sum of the electronic and zero-point energies.

The solvent effect (for DMSO) was simulated by performing self-consistent reaction field (SCRF) calculations. A continuum model – the integral equation formalism (IEF) version<sup>[29–31]</sup> of Tomasi's polarized continuum model (PCM)<sup>[32–34]</sup> – was used (applying the United Atom Topological Model). This approach defines the molecular cavity as the union of a series of interlocking spheres, centred on each of the distinct atoms of the molecule.

A calculation of the harmonic vibrational wavenumbers was carried out for all conformations (at the same level of theory) in order to check for minima in the potential energy surface and to obtain the theoretical vibrational pattern (both Raman and infrared) of the compounds in DMSO solution. Wavenumbers above  $400 \text{ cm}^{-1}$  were scaled by a factor of 0.9614<sup>[35]</sup> before comparing them with the experimental data, in order to correct for the anharmonicity of the normal modes of vibration.

## Results and Discussion

Similar to other phenolic systems and substituted benzaldehydes, alkyl phenolic esters predominantly exist as dimeric

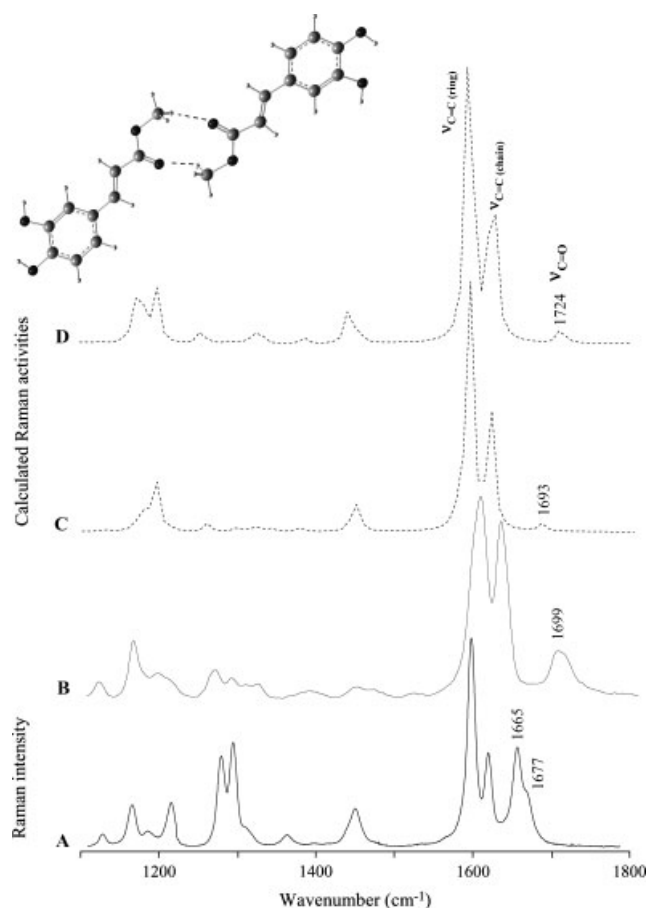


**Figure 2.** Raman spectra (1100–1800  $\text{cm}^{-1}$ , at 25 °C) for methyl caffeate (MC): experimental (solid line), in the solid state (A) and in  $2.0 \times 10^{-1} \text{ mol dm}^{-3}$  DMSO solution (B); calculated (B3LYP/6-31G\*\*, dotted line) for a DMSO solution (C) and for the isolated molecule (D). (The bands of the solvent are not shown. A representation of a proposed dimeric structure for MC is included).

structures in condensed phases, formed through stabilizing intermolecular  $(\text{C}=\text{O} \cdots \text{H}(\text{O}))$ ,  $(\text{H})\text{O} \cdots \text{H}_3(\text{C}-\text{O})_{\text{ester}}$ , and/or  $(\text{C}=\text{O} \cdots \text{H}_3(\text{C}-\text{O})_{\text{ester}})$  hydrogen bonds (Figs 2, 3 and Fig. S1, in Supporting Information).<sup>[15,16,19,36–39]</sup> For the investigated compounds, several dimeric entities were proposed to occur in the solid state and these were clearly detected by Raman spectroscopy.<sup>[16]</sup>

The monomer-to-dimer equilibrium, which determines the pharmaceutical activity of this type of esters, was evaluated for the caffeates and gallates under study by performing Raman spectroscopy titration experiments: room temperature spectra were obtained for DMSO solutions of the compounds, in the concentration range from  $1.0 \times 10^{-2}$  to  $1.0 \text{ mol dm}^{-3}$ , and the monomer/dimer ratio was determined for each system (through integration of the corresponding vibrational bands). DMSO was chosen as the solvent since it is commonly used for solubilizing this type of agents (similar to chemotherapeutic drugs such as cisplatin), as long as it is diluted in a physiological medium to a final concentration under 1% (in order to avoid cytotoxicity). Moreover, DMSO is Raman-transparent in the spectral region of interest (between *ca* 1500 and 1800  $\text{cm}^{-1}$ ), mostly affected by H-bonding, which renders it quite suitable for the present study.<sup>[15,19]</sup> Furthermore, any possible interactions between this solvent and the ester via  $(\text{O})\text{H} \cdots \text{O}(\text{C}=\text{S})$  close contacts (which would yield a characteristic band at about 1750  $\text{cm}^{-1}$ ) are known to occur

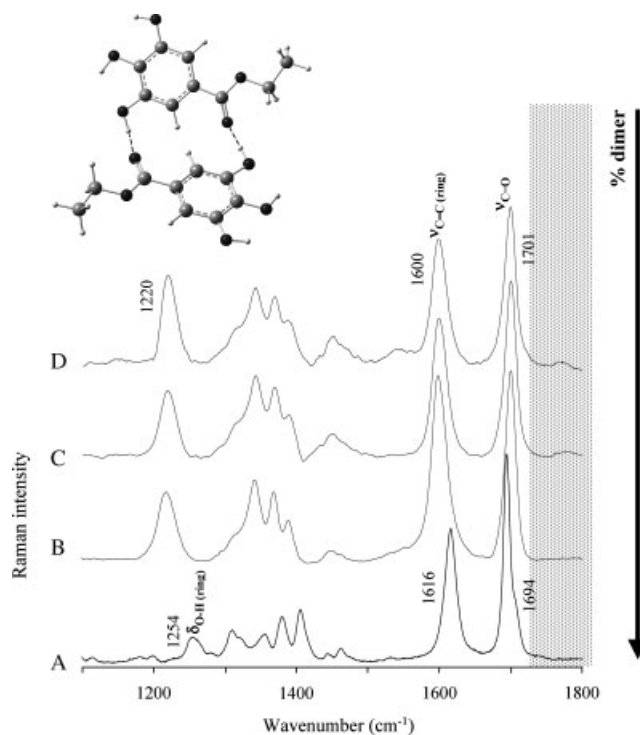


**Figure 3.** Experimental Raman spectra (1100–1800  $\text{cm}^{-1}$ , at 25 °C) for ethyl gallate (EG), in the solid state (A) and in  $1.0 \text{ mol dm}^{-3}$  (B),  $2.5 \times 10^{-1} \text{ mol dm}^{-3}$  (C) and  $1.0 \times 10^{-1} \text{ mol dm}^{-3}$  (D) DMSO solutions. (The bands of the solvent are not shown. A representation of a proposed dimeric structure for EG is included).

only for very high solvent/solute ratios<sup>[40]</sup> (much higher than the ones used in the present analysis). Consequently, significant intermolecular interactions apart from those between ester molecules (monomer-to-monomer) are ruled out, and Tomasi's SCRF continuum model constitutes a valid approach for the theoretical representation of these systems, since no explicit solvent molecules are necessary in order to accurately simulate the effect of the surrounding medium.

Tables 1 and 2 (and Tables S1–S4, in Supporting Information) comprise the experimental Raman wavenumbers (in the 1100–1800  $\text{cm}^{-1}$  range) and assignments for DMSO solutions of some of the caffeates and gallates studied, at distinct concentrations. These are compared with the data for the corresponding acids (caffeic<sup>[19]</sup> and gallic) and with the vibrational wavenumbers calculated for these systems. As a consequence of the presence of dimers, the  $\nu_{\text{C}=\text{O}}$  and  $\nu_{\text{OH}}$  modes were found to display a significant downward shift relative to the theoretically predicted values for the isolated molecules (free monomer entities), as expected according to the Raman results previously gathered for the solid esters,<sup>[16]</sup> and for the trihydroxylated analogue of EC, ethyl-3-(3,4,5-trihydroxyphenyl)-2-propenoate (ethyl caffeate, ethyl-3-(3,4,5-trihydroxyphenyl) (ETHPPE)).<sup>[15]</sup>

The dimeric and monomeric forms of the esters presently investigated are easily detected by Raman spectroscopy, since they were found, in accordance with previous studies on these phenolic systems,<sup>[15,16,19]</sup> to give rise to distinct vibrational features, namely in the regions comprising the  $\text{C}=\text{O}$  and  $\text{C}_{\text{ester}}-\text{O}$  stretchings and OH bending modes (*ca* 1100–1700  $\text{cm}^{-1}$ ), and the OH stretching bands (*ca* 3200–3500  $\text{cm}^{-1}$ ).<sup>[16]</sup> This is well evidenced in Figs 2 and 3 and Fig. S1 (in Supporting

**Table 1.** Experimental (1100–1800 cm<sup>-1</sup>) and calculated Raman wavenumbers (cm<sup>-1</sup>) for DMSO solutions of methyl caffeate (MC) and ethyl caffeate (EC). Values for 2.0 × 10<sup>-1</sup> mol.dm<sup>3</sup> DMSO solution of caffeic acid (CA) are included for comparison

CA Experimental 200 mM	MC				EC				Approximate description <sup>a</sup>
	Calculated <sup>b</sup>		Experimental		Calculated <sup>b</sup>		Experimental		
	Isolated molecule <sup>c</sup>	DMSO solution <sup>d</sup>	200 mM	20 mM	Isolated molecule <sup>c</sup>	DMSO solution <sup>d</sup>	200 mM	20 mM	
1688 <sup>e</sup>	1723	1693	1710 <sup>f</sup>	1698	1721	1681	1702 <sup>g</sup>	1701	$\nu(\text{C}=\text{O})$
1628	1630	1623	1634	1629	1629	1614	1633	1633	$\nu(\text{C}=\text{C})_{\text{chain}}$
1601	1599	1594	1608	1603	1599	1580	1607	1607	$\phi$ 8a
					1585	1571	1600		$\phi$ 8b + $\delta(\text{O}^{\text{B}}\text{H})$
1512	1511	1511	1518	1518	1512	1501	1518	1519	$\phi$ 19a + $\delta(\text{O}^{\text{B}}\text{H})$
	1452	1449	1474		1474	1469	1470		$\delta_{\text{as}}(\text{CH}_3) + \text{sciss}(\text{CH}_2)^*$
1447	1435	1437	1451		1435	1426	1446		$\phi$ 19b + $\delta_{\text{as}}(\text{CH}_3) + \text{sciss}(\text{CH}_2)^*$
1380	1373	1367	1392		1372	1359	1389		$\phi$ 3/14 + $\delta(\text{O}^{\text{7}}\text{H}) + \delta(\text{CH}) + \delta_{\text{s}}(\text{CH}_3)$
1321	1316	1328	1324		1315	1312	1320	1316	$\phi$ 3 + $\delta(\text{CH})_{\text{chain}} + \delta(\text{OH})_{\phi}$
1291	1305	1311	1293	1292	1306	1297	1292	1295	$\phi$ 14 + $\delta(\text{CH}) + \delta(\text{OH}) + \nu(\text{C}-\text{O})$
1257			1272	1273			1267	1267	$\nu(\text{C}-\text{O})$
	1233	1241	1212	1210	1233	1228	1210	1213	$\phi$ 3 + $\delta(\text{CH})_{\text{chain}} + \delta(\text{OH}) + \nu(\text{C}-\text{O})$
1185	1172	1187	1198	1197					$\phi$ 18a + $\delta(\text{O}^{\text{7}}\text{H})$
					1172	1160	1177	1179	$\delta(\text{CH}) + \delta(\text{OH}) + \nu(\text{C}-\text{O})$
1161	1155	1170	1168	1166			1164	1163	$\nu(\text{C}-\text{O}) + \delta(\text{CH})_{\text{chain}}$
1114	1128	1131	1124	1123	1128	1121	1122	1121	$\phi$ 18a + $\delta(\text{OH}) + r(\text{CH}_3)^{**}$

<sup>a</sup> Atoms are numbered according to Fig. 1(A). The Wilson notation was used for the description of benzene derivatives normal vibrations ( $\phi$ )<sup>[41,42]</sup>; for in-plane vibrations: C–C stretching vibrations (8a, 8b, 14, 19a, 19b), C–H/X bending vibrations (3, 18a, 18b), radial skeletal vibrations (1, 6a, 6b, 12), C–H stretching vibrations (2, 20a, 20b, 7a, 7b); for out-of-plane vibrations: C–H/X vibrations (5, 10a, 11, 17a, 17b), skeletal vibrations (4, 16a, 16b).  $\nu$  – stretching,  $\delta$  – in-plane deformation ( $\delta_{\text{s}}$  symmetric,  $\delta_{\text{as}}$  anti-symmetric),  $r$  – rocking, sciss. – scissoring. \*\* For caffeates. \* For ethyl caffeate.

<sup>b</sup> Calculated Raman wavenumbers are scaled by a factor of 0.9614.<sup>[35]</sup>

<sup>c</sup> From Ref. [20].

<sup>d</sup> At the SCRf-PCM/IEF level.

<sup>e</sup> Experimental  $\nu(\text{C}=\text{O})$  wavenumber for the solid: 1640 cm<sup>-1</sup>.<sup>[16]</sup>

<sup>f</sup> Experimental  $\nu(\text{C}=\text{O})$  wavenumbers for the solid: 1679, 1665 cm<sup>-1</sup>.<sup>[16]</sup>

<sup>g</sup> Experimental  $\nu(\text{C}=\text{O})$  wavenumbers for the solid: 1701, 1682, 1657 cm<sup>-1</sup> (unpublished data).

Information), which represent the experimental Raman spectra of DMSO solutions of MC, EC, and EG, respectively, at different concentrations.

For all the caffeates under study, a new band was detected in the solutions at about 1700 cm<sup>-1</sup>, as compared to the spectra of the solid compounds<sup>[16]</sup> (Tables 1, and 2, and Tables S1 and S2, in Supporting Information). This is ascribed to the C=O stretching vibration of the monomer, not involved in intermolecular H-bonding, which explains the expected shift to high wavenumbers (calculated value ca 1720 cm<sup>-1</sup><sup>[16,20]</sup>) relative to the  $\nu_{\text{C}=\text{O}}$  of the H-bonded carbonyl in the dimeric species (ca 1660–1680 cm<sup>-1</sup> in the solid.<sup>[16]</sup>) Actually, while the dimeric species is expected to be largely predominant in the solid, dilution is responsible for the presence of an increasing monomer population, giving rise to Raman bands due to the free carbonyl group (not implicated in intermolecular H-bonds). Although this effect was clearly observed for the caffeates in DMSO solution, the main band assigned to  $\nu_{\text{C}=\text{O}}$  for the solid gallates was also present in the solutions of the gallates. These trihydroxylated esters are therefore more prone to interact via intermolecular interactions in solution than the dihydroxylated cinnamates, probably due to the larger number of hydroxyl groups and to the smaller molecular volume (absence of the unsaturated pendant arm). The multiple bands present in the C=O stretching region for both DG and IPG in solution, in turn,

reflect the heterogeneity of those interactions (yielding dimeric structures), and it is a common feature of the condensed phase spectra of gallates (unpublished data).

In addition, comparison between the solution and the solid-state spectra clearly shows that the intensity of the chain  $\nu_{\text{C}=\text{C}}$  signal is significantly reduced in the condensed phase, in addition to the red shift detected for the  $\nu_{\text{C}=\text{O}}$  mode upon dimerisation. This can be explained by the conjugation between the C=O group (directly involved in the intermolecular hydrogen interaction) and the unsaturated pendant chain. In fact, this  $\pi$  system coupling due to intermolecular constraints will certainly affect the polarizability of the C=C oscillator, and consequently the Raman activity of its stretching mode, as previously verified in other phenolic systems.<sup>[43,44]</sup>

The spectral variations presently observed are easily understandable in the light of the proposed structures for the dimeric species formed by these alkyl phenolic esters<sup>[15,16]</sup> (Figs 2, 3 and Fig. S1, Supporting Information). The present data are also in agreement with the those reported for caffeic<sup>[17,19,45,46]</sup> and gallic acids,<sup>[47]</sup> which are well known for yielding stable dimeric structures in the solid phase.

The monomer-to-dimer population can be quantified through the intensity ratio between the  $\nu_{\text{C}=\text{O}}(\text{freemonomer})$  and the ring  $\nu_{\text{C}=\text{C}}$  bands, considering the latter as constant and the sole

**Table 2.** Experimental (1100–1800 cm<sup>-1</sup>) and calculated Raman wavenumbers (cm<sup>-1</sup>) for DMSO solutions of methyl gallate (MG) and ethyl gallate (EG). Values for a 2.0 × 10<sup>-1</sup> mol dm<sup>-3</sup> DMSO solution of gallic acid (GA) are included for comparison

GA Experimental 200 mM	MG				EG					Approximate description <sup>a</sup>
	Calculated <sup>b</sup>		Experimental		Calculated		Experimental			
	Isolated molecule <sup>c</sup>	DMSO solution <sup>d</sup>	500 mM	20 mM	Isolated molecule <sup>c</sup>	DMSO solution <sup>d</sup>	1000 mM	250 mM	20 mM	
1692 <sup>e</sup>	1723	1689	1705 <sup>f</sup>	1706	1719	1682	1699 <sup>g</sup>	1701	1700	$\nu(\text{C}=\text{O})$
1602	1608	1591	1600	1602	1608	1591	1599	1600	1602	$\phi 8b + 8a + \delta(\text{OH})$
					1515	1507			1543	$\phi 19a + \delta(\text{O}^7\text{H} + \text{O}^8\text{H})$
					1454	1443	1460		1485	sciss(CH <sub>2</sub> ) + $\delta_{as}(\text{CH}_3)$
					1443	1435	1449	1449		$r(\text{CH}_3)$
					1385	1379	1391	1390		$\omega(\text{CH}_2) + \delta_s(\text{CH}_3)$
	1366	1357	1366							$\phi 14 + \delta(\text{O}^7\text{H})$
1339	1357	1348	1355	1356	1367	1357	1369	1370		$\phi 13 + \delta(\text{O}^{14}\text{H}) + \omega(\text{CH}_2)^* + \delta_s(\text{CH}_3)^{**}$
					1342	1344	1342	1343		$\phi 2 + \delta(\text{O}^{14}\text{H}) + \omega(\text{CH}_2) + \delta_s(\text{CH}_3)$
	1272	1260	1251							$\phi 18b + \delta(\text{OH}) + \nu(\text{C}-\text{O})_{\text{ring}}$
1222	1220	1208	1226	1225	1213	1204	1218	1219	1215	$\nu(\text{C}-\text{O})_{\text{ester}} + \phi 18a + t(\text{CH}_2)^*$

<sup>a</sup> Atoms are numbered according to Fig. 1(B). The Wilson notation was used for the description of benzene derivatives normal vibrations ( $\phi$ )<sup>[41,42]</sup>; for in-plane vibrations: C–C stretching vibrations (8a, 8b, 14, 19a, 19b), C–H/X bending vibrations (3, 18a, 18b), radial skeletal vibrations (1, 6a, 6b, 12) C–H stretching vibrations (2, 20a, 20b, 7a, 7b); For out-of-plane vibrations: C–H/X vibrations (5, 10a, 11, 17a, 17b), skeletal vibrations (4, 16a, 16b).  $\nu$  – stretching,  $\delta$  – in-plane deformation ( $\delta_s$  symmetric,  $\delta_{as}$  anti-symmetric),  $t$  – twisting,  $r$  – rocking,  $\omega$  – wagging, sciss. – scissoring. \*\* For gallates. \* For ethyl gallate.

<sup>b</sup> Calculated Raman wavenumbers scaled by a factor of 0.9614.<sup>[35]</sup>

<sup>c</sup> At the B3LYP/6-31G\*\* level.

<sup>d</sup> At the SCRF-PCM/IEF level.

<sup>e</sup> Experimental  $\nu(\text{C}=\text{O})$  wavenumbers for the solid: 1695, 172 cm<sup>-1</sup>.<sup>[16]</sup>

<sup>f</sup> Experiment  $\nu(\text{C}=\text{O})$  wavenumbers for the solid: 1671, 1680, 1755 cm<sup>-1</sup>.<sup>[16]</sup>

<sup>g</sup> Experimental  $\nu(\text{C}=\text{O})$  wavenumbers for the solid: 1694, 1704, 1747 cm<sup>-1</sup> (unpublished data).

presence of monomer in the gas phase (e.g. calculated spectrum for the isolated molecule, Fig. 2). For EG, for instance, this ratio ranges from 1 in the gas, to 0.46 at 2 × 10<sup>-1</sup>, 0.39 at 1 × 10<sup>-1</sup>, 0.33 at 2 × 10<sup>-2</sup>, and 0.23 at 1.0 × 10<sup>-2</sup> mol dm<sup>-3</sup> (i.e. 77% of dimeric species).

## Conclusions

The Raman pattern in solution of several alkyl phenolic esters with potential pharmacological activity as antioxidant and chemopreventive agents against cancer (caffeates and gallates) was studied. The presence of dimeric species, previously reflected in the Raman data reported for the solid esters,<sup>[16]</sup> was also clearly evidenced in the spectra presently obtained for DMSO solutions, namely through the characteristic low wavenumber shifts detected for the  $\nu_{\text{C}=\text{O}}$ ,  $\nu_{\text{C}-\text{O}}$  and  $\nu_{\text{O}-\text{H}}$  modes upon increase of the dimeric form (intermolecular H-bond formation).

The dimer-to-monomer equilibrium was monitored through comparison of the vibrational spectra of the solid and progressively diluted esters, which revealed the effect of a continuous decrease of the dimer/monomer ratio and allowed the identification of the main spectral changes associated to the dimerization process – mainly in the  $\nu_{\text{C}=\text{O}}$ ,  $\nu_{\text{C}-\text{O}}$ ,  $\nu_{\text{O}-\text{H}}$  and  $\delta_{\text{OH}}$  bands. The percentage of dimeric versus monomeric species was determined as a function of concentration. For each ester and concentration tested, a tentative quantification of the dimer/monomer fraction was undertaken.

These results will enable the identification of the species present in a particular pharmacological formulation of a phenolic ester

(thus predicting its activity), simply by recording its Raman spectrum and analysing particular wavenumber regions (thus yielding a fingerprint for each compound and each concentration). In fact, this spectroscopic technique is becoming more and more popular as a reliable and non-invasive method for the identification and characterization of pharmaceutically relevant compounds.

## Supporting information

Supporting information may be found in the online version of this article.

## Acknowledgements

The authors acknowledge financial support from the Portuguese Foundation for Science and Technology–Project POCI/QUI/55631/2004 (co-financed by the European Community fund FEDER) and PhD fellowships SFRH/BD/16520/2004 and SFRH/BD/40235/2007.

## References

- [1] A. Trichopoulou, P. Lagiou, A. M. Pappas, *Antioxidant Status, Diet, Nutrition and Health*, CRC Press: Boca Raton, **1999**.
- [2] S. D. Ray, D. Bagchi, *Phytopharmaceuticals in Cancer Chemoprevention – 22. Roles of Polyphenols, Flavonoids and Oligomeric Proanthocyanidins in Cancer Chemoprevention*, Taylor & Francis: London, **2004**, pp 311.
- [3] N. N. Sailendra, T. G. Taruscio, D. L. Barney, J. H. Exon, *Crit. Rev. Food Sci. Nutr.* **2006**, *46*, 161.
- [4] N. Chi Che, T. A. N. Kong, *Free Radic. Biol. Med.* **2004**, *36*, 1505.

- [5] B. Bharat, A. Aggarwal, S. Shishodia, *Biochem. Pharmacol.* **2006**, *71*, 1397.
- [6] P. Fresco, F. Borges, C. Diniz, M. P. M. Marques, *Med. Res. Rev.* **2006**, *26*, 747.
- [7] C. A. Gomes, T. G. da Cruz, J. L. Andrade, N. Milhazes, F. Borges, M. P. M. Marques, *J. Med. Chem.* **2003**, *46*, 5401.
- [8] M. A. S. Silva, C. M. M. Santos, J. A. S. Cavaleiro, H. R. Tavares, F. Borges, F. A. M. Silva, *NMR Studies on the Antiradical Mechanism of Phenolic Compounds Towards 2,2-Diphenyl-1-picrylhydrazyl Radical; Magnetic Resonance in Food Science – A View to the Next Century*, Royal Society of Chemistry: London, **2001**.
- [9] F. Borges, J. Lima, I. Pinto, S. Reis, C. Siquet, *Helv. Chim. Acta* **2003**, *86*, 3081.
- [10] M. Esteves, C. Siquet, A. Gaspar, V. Rio, J. B. Sousa, S. Reis, M. P. M. Marques, F. Borges, *Arch. Pharm.* **2008**, *341*, 164.
- [11] M. P. M. Marques, F. Borges, J. Sousa, R. Calheiros, J. Garrido, A. Gaspar, F. Antunes, C. Diniz, P. Fresco, *Letts. Drugs Des. Discov.* **2006**, *3*, 316.
- [12] C. Siquet, F. Paiva-Martins, N. Milhazes, J. L. F. C. Lima, S. Reis, F. Borges, *Free Radic. Res.* **2006**, *40*, 433.
- [13] F. A. M. Silva, F. Borges, C. Guimaraes, J. Lima, C. Matos, S. Reis, *J. Agric. Food Chem.* **2000**, *48*, 2122.
- [14] S. M. Fiuza, C. Gomes, L. J. Teixeira, M. T. G. da Cruz, M. Cordeiro, N. Milhazes, F. Borges, M. P. M. Marques, *Bioorg. Med. Chem.* **2004**, *12*, 3581.
- [15] J. B. Sousa, R. Calheiros, V. Rio, F. Borges, M. P. M. Marques, *J. Mol. Struct.* **2006**, *783*, 122.
- [16] R. Calheiros, N. F. L. Machado, S. M. Fiuza, A. Gaspar, J. Garrido, N. Milhazes, F. Borges, M. P. M. Marques, *J. Raman Spectrosc.* **2008**, *39*, 95.
- [17] E. Van Besien, M. P. M. Marques, *J. Mol. Struct. (Theochem)* **2003**, *625*, 265.
- [18] S. M. Fiuza, E. Van Besien, N. Milhazes, F. Borges, M. P. M. Marques, *Bioorg. Med. Chem.* **2004**, *12*, 3581.
- [19] S. M. Fiuza, E. Van Besien, N. Milhazes, F. Borges, M. P. M. Marques, *J. Mol. Struct.* **2004**, *693*, 103.
- [20] N. F. L. Machado, R. Calheiros, S. M. Fiuza, F. Borges, A. Gaspar, J. Garrido, M. P. M. Marques, *J. Mol. Model.* **2007**, *13*, 865.
- [21] F. A. M. Silva, F. Borges, M. Ferreira, *J. Agric. Food Chem.* **2001**, *49*, 3936.
- [22] M. J. Frisch, G. W. Trucks, H. B. Schlegel, G. E. Scuseria, M. A. Robb, J. R. Cheeseman, J. A. Montgomery Jr, T. Vreven, K. N. Kudin, J. C. Burant, J. M. Millam, S. S. Iyengar, J. Tomasi, V. Barone, B. Mennucci, M. Cossi, G. Scalmani, N. Rega, G. A. Petersson, H. Nakatsuji, M. Hada, M. Ehara, K. Toyota, R. Fukuda, J. Hasegawa, M. Ishida, T. Nakajima, Y. Honda, O. Kitao, H. Nakai, M. Klene, X. Li, J. E. Knox, H. P. Hratchian, J. B. Cross, V. Bakken, C. Adamo, J. Jaramillo, R. Gomperts, R. E. Stratmann, O. Yazyev, A. J. Austin, R. Cammi, C. Pomelli, J. W. Ochterski, P. Y. Ayala, K. Morokuma, G. A. Voth, P. Salvador, J. J. Dannenberg, V. G. Zakrzewski, S. Dapprich, A. D. Daniels, M. C. Strain, O. Farkas, D. K. Malick, A. D. Rabuck, K. Raghavachari, J. B. Foresman, J. V. Ortiz, Q. Cui, A. G. Baboul, S. Clifford, J. Cioslowski, B. B. Stefanov, G. Liu, A. Liashenko, P. Piskorz, I. Komaromi, R. L. Martin, D. J. Fox, T. Keith, A. M. Al-Laham, C. Y. Peng, A. Nanayakkara, M. Challacombe, P. M. W. Gill, B. Johnson, W. Chen, M. W. Wong, C. Gonzalez, J. A. Pople, *Gaussian 03, Revision B.04*, Gaussian: Pittsburgh, **2003**.
- [23] C. Lee, W. Yang, R. G. Parr, *Phys. Rev.* **1988**, *B37*, 785.
- [24] B. Miehllich, A. Savin, H. Stoll, H. Preuss, *Chem. Phys. Lett.* **1989**, *157*, 200.
- [25] A. Becke, *Phys. Rev.* **1988**, *A38*, 3098.
- [26] A. J. Becke, *J. Chem. Phys.* **1993**, *98*, 5648.
- [27] G. A. Petersson, A. Bennett, T. G. Tensfeldt, M. A. Al-Laham, W. A. Shirley, J. Mantzaris, *J. Chem. Phys.* **1988**, *89*, 2193.
- [28] C. Peng, P. Y. Ayala, H. B. Schlegel, M. J. Frisch, *J. Comput. Chem.* **1996**, *17*, 49.
- [29] E. Cancès, B. Mennucci, J. Tomasi, *J. Chem. Phys.* **1997**, *107*, 3032.
- [30] B. Mennucci, E. Cancès, J. Tomasi, *J. Phys. Chem. B* **1997**, *101*, 10506.
- [31] E. Cancès, B. J. Mennucci, *J. Math. Chem.* **1998**, *23*, 309.
- [32] V. Barone, M. Cossi, J. Tomasi, *J. Comput. Chem.* **1998**, *19*, 404.
- [33] R. Cammi, J. Tomasi, *J. Comput. Chem.* **1995**, *16*, 1449.
- [34] S. Mieltus, E. Scrocco, J. Tomasi, *J. Chem. Phys.* **1981**, *55*, 117.
- [35] A. P. Scott, L. Radom, *J. Phys. Chem.* **1996**, *100*, 16502.
- [36] P. J. A. Ribeiro-Claro, L. A. E. Batista de Carvalho, A. M. Amado, *J. Raman Spectrosc.* **1997**, *28*, 867.
- [37] L. Pálíčko, *Acta Crystallogr.* **1999**, *B55*, 216.
- [38] J. T. Kiss, K. Felföldi, T. Kortvelyesi, I. Palinko, *Vib. Spectrosc.* **2000**, *22*, 63.
- [39] M. P. M. Marques, A. M. Amorim da Costa, P. J. A. Ribeiro-Claro, *J. Phys. Chem. A* **2001**, *105*, 5292.
- [40] P. Novak, D. Vikić-Topić, Z. Meić, S. Sekusak, A. J. Sabljic, *J. Mol. Struct.* **1995**, *356*, 131.
- [41] E. B. Wilson Jr, *Phys. Rev.* **1934**, *45*, 706.
- [42] G. Varsányi, *Assignments for Vibrational Spectra of Seven Hundred Benzene Derivatives; Akadémiai Kiadó, Budapest/Adam Hilger Limited: London*, **1974**.
- [43] E. D. J. Becker, *J. Phys. Chem.* **1991**, *95*, 2818.
- [44] H. M. Badawi, W. J. Forner, *J. Mol. Struct. (Theochem)* **2004**, *677*, 153.
- [45] S. Sánchez-Cortés, J. V. García-Ramos, *Spectrochim. Acta* **1999**, *A55*, 2935.
- [46] S. Sánchez-Cortés, J. V. García-Ramos, *Appl. Spectrosc.* **2000**, *54*, 230.
- [47] S. Sánchez-Cortés, J. V. García-Ramos, *J. Colloid Interface Sci.* **2000**, *231*, 98.